

Direction-of-Arrival Assisted Sequential Spoofing Detection and Mitigation

Michael Meurer^{1,2}, Andriy Konovaltsev², Manuel Appel^{1,2}, Manuel Cuntz^{1,2}

Email: {Michael.Meurer, Andriy.Konovaltsev, Manuel.Appel, Manuel.Cuntz}@dlr.de

¹ Chair of Navigation, RWTH Aachen University, Germany

² German Aerospace Center (DLR), Germany

BIOGRAPHIES

Dr. Michael Meurer received the diploma in electrical engineering and the Ph.D. degree from the University of Kaiserslautern, Germany. After graduation, he joined the Research Group for Radio Communications at the Technical University of Kaiserslautern, Germany, as a senior key researcher, where he was involved in various international and national projects in the field of communications and navigation both as project coordinator and as technical contributor. From 2003 till 2013, Dr. Meurer was active as a senior lecturer and Associate Professor (PD) at the same university. Since 2006 Dr. Meurer is with the German Aerospace Centre (DLR), Institute of Communications and Navigation, where he is the director of the Department of Navigation and of the center of excellence for satellite navigation. In addition, since 2013 he is a professor of electrical engineering and director of the Chair of Navigation at the RWTH Aachen University. His current research interests include GNSS signals, GNSS receivers, interference and spoofing mitigation and navigation for safety-critical applications.

Dr. Andriy Konovaltsev received his engineer diploma and the Ph.D. degree in electrical engineering from Kharkov State Technical University of Radio Electronics, Ukraine in 1993 and 1996, respectively. He joined the Institute of Communications and Navigation of DLR in 2001. His main research interest is in application of antenna array signal processing for improving performance of satellite navigation systems in challenging signal environments.

Manuel Appel received his diploma degree in electrical engineering from the university of applied science Ingolstadt, Germany in 2008. Additionally he received a M.Sc. degree from Technical University Munich in 2013 after working at Fraunhofer Institute for Integrated Circuits in Erlangen. He joined the Institute of Communications and Navigation of DLR in January 2014. His main research interest is in development of signal processing algorithms for robust GNSS receivers with the main focus on spoofing detection and mitigation.

Manuel Cuntz received the diploma in electrical engineering degree in 2005 from the Technical University of Kaiserslautern. He joined the Institute of Communications and Navigation of DLR in June 2006. His fields of research are multi-antenna satellite navigation receivers.

ABSTRACT

The paper presents several novel techniques for detection of spoofing/meaconing signals using the direction-of-arrival (DOA) measurements available in a multi-antenna navigation receiver. The detection is based on comparison and statistically testing of the measured DOAs against the expected DOAs. The expected DOAs are computed in the receiver using the almanac and ephemeris. The attitude of the antenna array is assumed to be unknown and therefore has to be estimated as part of a joint spoofing detection/estimation problem. It is shown that the statistics of the DOA estimation error for a signal heavily depends on the elevation of the relevant satellite in the local antenna coordinate system. Therefore, an extended technique for joint spoofing detection and attitude estimation is proposed which incorporates signal and elevation specific statistical information about DOA errors. The performance of the new approach is analyzed through simulations. An extension of the developed snapshot based approach to a sequential approach is proposed. It is shown that new sequential techniques offer great potential for increasing the performance of joint spoofing detection and attitude estimation compared to snapshot based techniques while at the same time the complexity can be significantly reduced.

I. Introduction

The threat of spoofing attacks is a serious problem for civil GNSS applications with safety content, such as airplane landing or ship navigation in a harbor [1] [13]. Also many strategically important infrastructures such as electric power grids or mobile communications networks are becoming increasingly dependent on GNSS services. In contrast to

military GNSS users which solve the problem to a large extent by utilizing encrypted signals, civil GNSS receivers have to live today and most probably in the near and mid future with unencrypted signals of open GNSS services. Therefore, such receivers have to be protected by additional receiver-sided techniques, which are able to detect and mitigate spoofing attacks.

Adequate solutions for the GNSS spoofing problem are subject of intensive research, see e.g. [1][2][5][6][7][14][15][16]. A number of receiver-autonomous spoofing detection techniques have been proposed. In order to detect the presence of a spoofing attack these techniques rely on the observation of the signal power [1], the Doppler frequency offset [5], the PRN code delay and its change rate [1][6], the correlation function shape as well as the cross-correlation of the signal components at different carrier frequencies [1][5][6]. The advanced protection against even the most sophisticated spoofing attacks can be provided by the use of multiple antennas [7]. This comes from the fact that the differential carrier phases of a signal observed at different antennas depend on the direction of arrival of the signal. Using this, a receiver with an antenna array is able to estimate the directions of arrival of the GNSS signals [8] and detect the spoofing attack if unexpected directions of arrival occur - especially if a large part of the signals come from a single direction [2]. Moreover the malicious signals can be mitigated by generating a spatial zero in the array antenna reception pattern in the direction of the spoofing source.

The use of the multi-antenna based approach for spoofing detection and mitigation was investigated by the authors of this paper in [2][3][4] and is shortly reviewed in Section II of this paper. A technique for joint spoofing detection and antenna attitude estimation was developed which uses estimated signal directions of arrival. The detection is based on testing the observed directions-of-arrival (DOAs) of the satellite signals against the predicted DOAs. The latter are computed while solving for the user position, velocity and time (PVT). This is due to the fact that the direction of arrival of a satellite signal is required to calculate the corresponding errors corrections for the signal delay in ionosphere and troposphere. To estimate the direction to the satellite, the PVT module of the user receiver makes use of the ephemeris information in the navigation message and the latest user position estimate. These predicted DOAs are obtained in the user local east-north-up (ENU) coordinates. Because the attitude of the antenna array in the local ENU coordinates is not necessarily known, the spoofing detection is treated as a joint detection (i.e. of spoofing attack) and estimation (i.e. of attitude) problem. The main challenge in this process is to exploit antenna attitude information for reliable spoofing detection and at the same time to ensure that spoofed signals do not have any impact on the attitude estimation. In order to achieve this goal the approach analyzes within the joint spoofing detection and attitude estimation optimization

problem several hypotheses about unspoofed subsets of all received signals and follows decision metrics which are similar to receiver autonomous integrity monitoring (RAIM) in order to identify the authentic signals [2].

The accuracy of direction-of-arrival estimation in planar antenna arrays is highly elevation dependent. Moreover, due to electromagnetic coupling between antenna elements the estimation accuracy of DOAs may also heavily vary over azimuth. The latter applies especially for miniaturized antenna arrays with antenna element spacing well below half of the wavelength of the used radio waves. Such antenna arrays are of high interest in mobile applications, since they have a similar size and form factor as conventional antennas (e.g. ARINC antenna form factor in aeronautics).

The techniques developed in [2][3][4] suffer from the effect that they are snapshot based and cannot cope with the direction dependent estimation quality of DOAs. This leads to suboptimal estimation results for attitude and spoofing detection. This paper presents a novel, non-iterative and optimal approach for joint spoofing detection and attitude estimation which takes the different qualities of input data into account. For that purpose the directional dependency of DOA estimation errors in typical scenarios is characterized by analyzing measurement data.

In typical scenarios in mobility on land, on sea and in the air, the attitude of the user platform (e.g. vehicle, ship, aircraft) does not change suddenly but with limited turn rates and turn rate changes. Therefore, the knowledge about attitude in a certain epoch can be exploited for the attitude estimation in following epochs as a priori knowledge. In this paper, the aforementioned snapshot based technique will be further extended to a new sequential technique for joint spoofing detection and attitude estimation which exploits the limited changes in attitude.

It is quite likely that a spoofing scenario does not change suddenly from epoch to epoch, e.g. that for several consecutive epochs the same signals can be expected to be affected by spoofing. In this case, the knowledge from one epoch about subsets of trustful/authentic signals (and spoofed signals, respectively) can be exploited as a priori information in following epochs. The paper introduces an extension to the new sequential technique proposed above which exploits this a priori information. This approach allows significantly reducing the complexity of the overall technique since the average number of hypothesis to follow can be significantly reduced while at the same time the probability of correct spoofing detection is not affected.

The paper is organized as follows: In the following section the basic idea of joint attitude estimation and spoofing detection is revisited and the relevant signal model is introduced. In Section III the dependency of the DOA estimation error with respect to the DOA to be estimated is

analyzed. It is shown that an elevation dependency of the estimation error has to be considered. In Section IV benefit is taken of the elevation dependent error model and an improved approach for joint attitude estimation and spoofing detection is proposed. In Section V the new approach is extended from snapshot based processing to sequential processing. Finally, Section VI concludes the paper.

The investigations are performed using a vector-matrix notation. Vectors and matrices are printed in bold face using lower case and upper case letters, respectively. In the analysis $\|\cdot\|$ denotes the Euclidean norm of the vector or matrix in brackets and estimated quantities are marked by “^” (hat).

II. Antenna Based Joint Attitude Estimation and Spoofing Detection Revisited

The spoofing detection technique introduced in [2][3][4] is based on the discrimination between the counterfeit and authentic GNSS signals by using the information about the directions of arrival of these signals. The detection process requires two pieces of such information (see Fig. 1). The first piece is the estimation of the actual DOAs by using one of suitable array signal processing algorithms [9][10]. These DOA measurements, usually in form of azimuth and elevation angles, refer to the local coordinate frame of the antenna array.

The second piece of the directional information is obtained as a side product of the receiver positioning solution. Once the user position is estimated, a set of unit vectors $\{\mathbf{a}_n\}_{n=1}^N$, $\mathbf{a}_n \in \mathbb{R}^{3 \times 1}$ pointing from the user to each of N visible navigation satellites with valid ephemeris can be computed in the local geodetic east-north-up (ENU) coordinate frame. The effect of the positioning error on the vectors $\{\mathbf{a}_n\}_{n=1}^N$ can be neglected due to the large ranges to the MEO orbit navigation satellites.

Without loss of generality it will be further assumed that the antenna coordinates and the local ENU frames have the same origin but are generally not aligned, e.g. the antenna coordinates can be seen as a rotated version of the ENU frame. This rotation is characterized by the corresponding Euler angles roll r , pitch p and yaw y angles, which characterize the attitude of the antenna platform, see for example [11] for more details. Considering first an ideal case of error-free DOA measurements, the axis rotation matrix can be described as follows

$$\mathbf{b}_n = \mathbf{R}(r, p, y)\mathbf{a}_n, \quad 1 \leq n \leq N, \quad (1)$$

where $\mathbf{b}_n \in \mathbb{R}^{3 \times 1}$ is a unit vector pointing to the n th satellite in the antenna local coordinates, while $\{\mathbf{b}_n\}_{n=1}^N$ being the entire set of the error-free DOA measurements, and

$\mathbf{R}(r, p, y) \in SO(3) \subset \mathbb{R}^3$ is the rotation matrix. This matrix is unitary, i.e. $\mathbf{R}^T \mathbf{R} = \mathbf{I}$, and its elements are determined by the Euler angles [11].

Since in practice the n -th DOA measurement is a noise-corrupted estimate $\hat{\mathbf{b}}_n$ of \mathbf{b}_n , an additional rotation matrix \mathbf{R}_n^N describing the DOA measurement error should be introduced

$$\hat{\mathbf{b}}_n = \mathbf{R}_n^N \mathbf{R}(r, p, y)\mathbf{a}_n, \quad 1 \leq n \leq N. \quad (2)$$

As addressed in [2][3][4] the maximum likelihood estimation of the rotation matrix $\hat{\mathbf{R}}$ can be obtained by minimizing the distance between $\hat{\mathbf{b}}_n$ and \mathbf{b}_n as follows

$$\hat{\mathbf{R}} = \arg \min_{\forall r, p, y} \sum_{n=1}^N \|\mathbf{R}(r, p, y)\mathbf{a}_n - \hat{\mathbf{b}}_n\|^2 \quad (3)$$

or by using a matrix notation for each set of DOA unit vectors

$$\hat{\mathbf{R}} = \arg \min_{\forall r, p, y} \|\mathbf{R}(r, p, y)\mathbf{A} - \hat{\mathbf{B}}\|^2 \quad (4)$$

where $\mathbf{A} = [\mathbf{a}_1, \dots, \mathbf{a}_N]$, $\mathbf{A} \in \mathbb{R}^{3 \times N}$ and $\hat{\mathbf{B}} = [\hat{\mathbf{b}}_1, \dots, \hat{\mathbf{b}}_N]$, $\hat{\mathbf{B}} \in \mathbb{R}^{3 \times N}$.

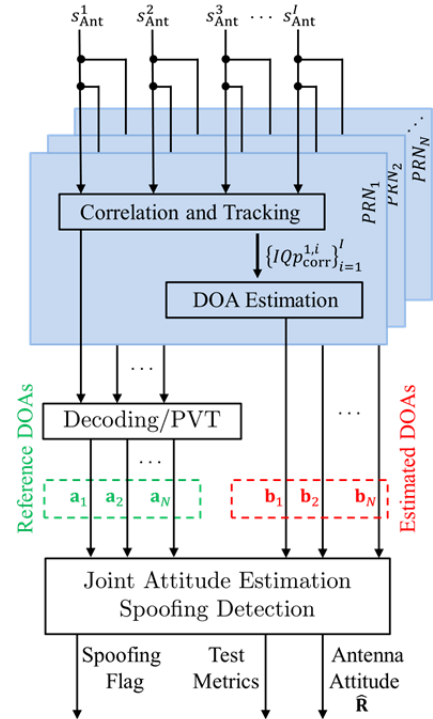


Fig. 1 Receiver architecture used for spoofing detection

The least squares problem formulated by (4) is known in the literature as the Wahba's problem. A computationally effective solution of the problem is available using the singular value decomposition (SVD) technique [12].

As proposed in [3] the quality of the solution for the antenna attitude can be assessed using the sum of squares of errors (SSE) test statistics in a similar way as within receiver autonomous integrity monitoring (RAIM) techniques. The SSE metric is defined as follows

$$SSE = \text{trace}\{[\mathbf{R}(r, p, y)\mathbf{A} - \hat{\mathbf{B}}]^T \mathbf{R}_N^{-1} [\mathbf{R}(r, p, y)\mathbf{A} - \hat{\mathbf{B}}]\}, \quad (5)$$

where the inverse of the covariance matrix of the measurement noise \mathbf{R}_N^{-1} is used for normalizing individual residuals of the least squares solution. In [3] it is assumed that the individual DOA measurement errors $\hat{\mathbf{b}}_n - \mathbf{b}_n$ are Gaussian and not correlated with each other and the matrix \mathbf{R}_N is a diagonal matrix consisting of the error variances $\sigma_1^2, \sigma_2^2, \dots, \sigma_N^2$. If no systematic offsets are observed between the measured and predicted DOAs of the GNSS signals – i.e. if no spoofing is present – the SSE metric defined by (5) follows a central chi-squared distribution with $k = (2N - 3)$ degrees of freedom. In the complementary case, if all or some of the measured DOAs are biased with respects to predicted DOAs – i.e. if spoofing is present – the SSE metric follows a non-central chi-squared distribution with the same number of degrees of freedom as above but with some non-zero non-centrality parameter λ :

$$\begin{aligned} H_0(\text{no error}): SSE &\sim \chi^2(k) \\ H_1(\text{error}): SSE &\sim \chi'^2(k, \lambda) \\ k &= (2N - 3) \\ \lambda &= \sum_{n=1}^N \left(\frac{\Delta_n}{\sigma_n}\right)^2 \end{aligned} \quad (6)$$

where

Δ_n is the bias in the n -th DOA measurement, this bias is expressed as a spatial angle ψ_n between two direction cosines vectors of the measured DOA $\hat{\mathbf{b}}_n$ and the predicted ‘‘almanac’’ DOA \mathbf{b}_n :

$$\Delta_n = \psi_n = \arccos \langle \hat{\mathbf{b}}_n, \mathbf{b}_n \rangle, \quad (7)$$

σ_n is the standard deviation of the n -th DOA measurement error given in units of the spatial angle ψ_n .

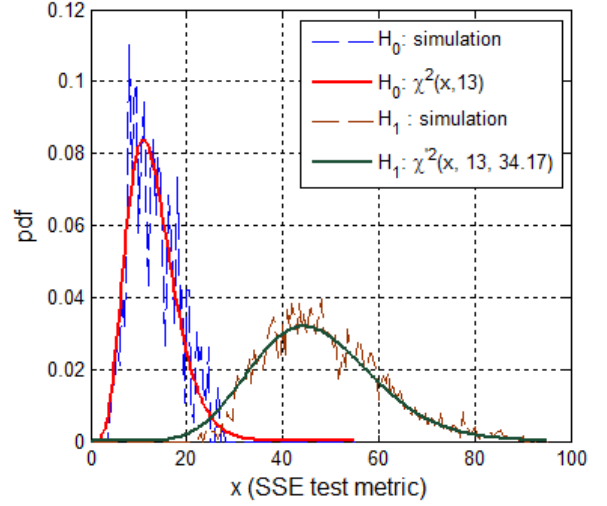


Fig. 2 Pdfs of SSE test metric of (5) for H_0 and H_1 hypotheses

An example of probability density functions (pdfs) of the SSE test statistics for H_0 and H_1 hypothesis are shown in Fig. 2. These numerical results were obtained by Monte Carlo simulations of DOA measurements for seven GNSS satellites [3]. In simulations for the H_1 case, a single bias was introduced into the fifth DOA measurement: $\Delta_5 = 12.5^\circ$ so that $(\Delta_5/\sigma_5)^2 = 34.17$.

As can be observed in Fig. 2, the detection of the systematic biases in DOA measurements can be performed by using standard fixed alarm rate hypothesis testing, i.e. by setting a threshold for the SSE test metric defined by some desired false alarm rate. The presence of the systematic biases can then serve as one of indications of spoofer / meaconing attacks.

In [2] it is shown how a reliable identification of all spoofed signals can be performed based on above explained hypotheses testing. In a systematic way all possible hypotheses about spoofed subsets of satellite signals are analyzed and the largest unspoofed subset of satellite signals is identified.

III. Direction Of Arrival Estimation and Estimation Error Model

A. Methodology for DOA Estimation Error Analysis

The estimation approach of (4) which was revisited in Section II and introduced in [2][3][4] is based on several implicit assumptions about the statistics of the DOA estimation errors. One of the most important assumptions is that the error vector $\hat{\mathbf{b}}_n - \mathbf{b}_n$ is white Gaussian distributed with equal distribution for all satellite signals $n = 1 \dots N$, i.e. it is assumed that each DOA is estimated with equal quality and isotropic error behaviour.

These assumptions are made for sake of simplicity and are driven by the need to keep the mathematical derivations traceable. However, in reality due to physical limits it is in question how far these assumptions hold. The accuracy of direction-of-arrival estimation in planar antenna arrays is highly elevation dependent. Due to electromagnetic coupling between antenna elements the estimation accuracy of DOAs may also heavily vary over azimuth. The latter applies especially for miniaturized antenna arrays with antenna element spacing well below half of the wavelength of the used radio waves. Moreover, the resolution of DOA estimation in planar arrays may differ for the azimuth and elevation component.

In order to clarify these questions about the DOA estimation error statistics real measurement data was captured with a multi antenna setup and processed in order to determine DOA estimation error statistics. The data was captured using the multi antenna GNSS receiver GALANT of the German Aerospace Center (DLR), see Fig. 3 a. This receiver was developed by DLR for applications with safety of life content. The receiver performs individual beamforming and performs direction of arrival (DOA) estimation after the correlation process for all tracked satellites. The real-time receiver is described in detail in [8]. For investigating the direction of arrival estimation error and its statistics the 2-by-2 rectangular adaptive antenna of the DLR GALANT receiver was mounted on the roof of the building of the DLR Institute of Communications and Navigation in Oberpfaffenhofen, Germany (see Fig. 3 b). The DLR receiver makes use of a two-dimensional Unitary ESPRIT algorithm [9][10] for DOA estimation. This choice is motivated by the high computational efficiency of this super resolution technique, which makes it attractive for real-time application, and the ability to separate coherent signals by using forward-backward averaging, which is helpful to cope with multipath. The 2D Unitary ESPRIT algorithm is implemented in the baseband software of the receiver in the post-correlation part of the signal processing chain.

Blocks of the array signal data were collected in each multi-antenna satellite tracking channel and used in the post-processing by a direction finding technique. The data blocks were collected simultaneously for 12 satellites signals being tracked by the receiver. Each array signal sample consists of complex-value outputs of four prompt PRN-code correlators. A single data block corresponds to the 20 ms of observation time.

B. Analysis Results and Error Model

In order to evaluate the characteristics of the DOA estimation error, the corresponding measurements of the GALANT receiver have been continuously recorded over 48 hours. For each epoch within this time the DOA measurement of every tracked satellite signal has been performed using the ESPRIT

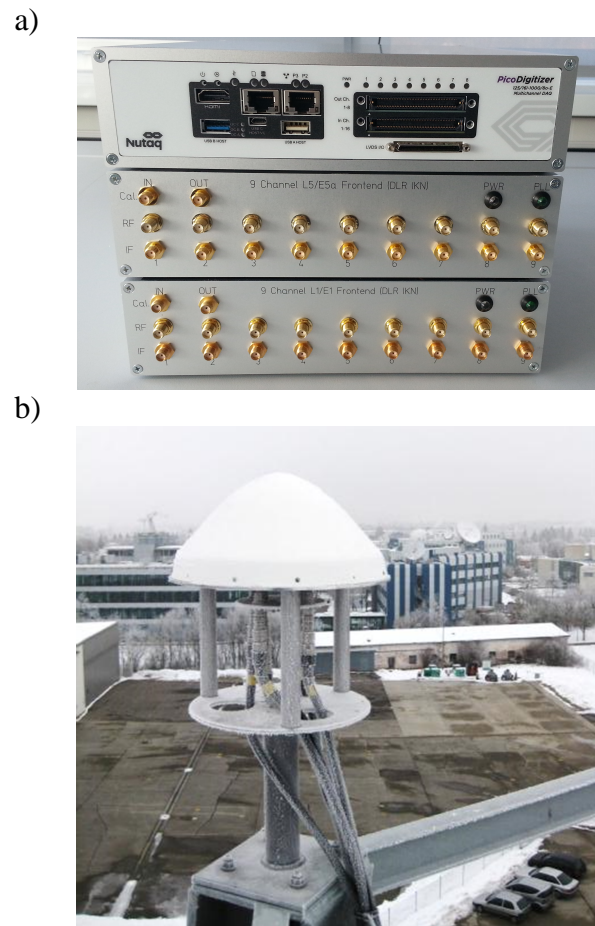


Fig. 3 View on (a) GALANT multi-antenna receiver and (b) antenna array roof installation

algorithm. The reference DOAs for the error calculation have been obtained by using a long-time average of the attitude of the GALANT antenna and the satellite ephemeris information. The DOA estimation error is then determined as the enclosed angle between the measured and the reference DOAs.

Fig. 6 gives an overview of the achieved results. As a function of azimuth and elevation of the considered satellite signal measured in the local antenna coordinate frame, the angular root mean square error (RMSE) of the DOA estimation is depicted. The individual plot for the azimuth and elevation components of the DOA estimation errors are shown in Fig. 4.

On the one hand it can be observed that a strong dependency between estimation error and elevation angle exists. On the other hand, the dependency of the DOA estimation error on azimuth turns out to be minor. Since the used antenna array is a planar array the result is not surprising. Due to physical limits the resolution of DOA estimation for very low elevations, i.e. for grazing incidence of the wave, is much

lower than for high elevations, i.e. for boresight reception. Since the antenna pattern of the antenna array does not show a significant dependency over azimuth [8] also no significant dependency of the DOA estimation errors can be observed. However, when using antenna arrays which are even more miniaturized with significant electromagnetic coupling effects among the antenna elements also a more dominant azimuth dependency could be expected.

Within this paper we put our focus on the dependency of the DOA estimation error on the elevation within the local antenna coordinate frame and neglect the minor dependency on the azimuth. Setting out from this observation we analyze the DOA estimation error with respect to its components in elevation and azimuth direction. Fig. 5 shows the results for the entire data set as a function of elevation both for the azimuth and the elevation component. Several observations can be made:

- 1) Azimuth and elevation component follow different statistics with respect to the distribution of the DOA error. The typical error of the azimuth component is smaller than the error in the elevation component.

- 2) The elevation dependency of the elevation component is significant. Especially for low elevations up to 30° the estimation error is significantly higher than for higher elevations.
- 3) The error distribution of the azimuth component is almost independent of the elevation. Only for very high elevations above 80° the error in the azimuth component seems to be higher. However, this result is caused by the natural effect of convergent lines of longitude for high elevations.

Neglecting the azimuthal dependency and using the measurement results presented in Fig. 4 a simple over-bounding Gaussian model for the angular DOA estimation error can be derived as follows:

$$\sigma_{\text{RMS}}(\theta) = \sigma_{90} \cdot \alpha_N \cdot \left(\alpha_1 + K e^{-\alpha_2 \frac{\theta}{\text{degree}}} \right) \quad (8)$$

$$\alpha_1 = 0.175, \alpha_2 = 0.0436,$$

$$\alpha_N = (\alpha_1 + K e^{-\alpha_2 \cdot 90})^{-1}.$$

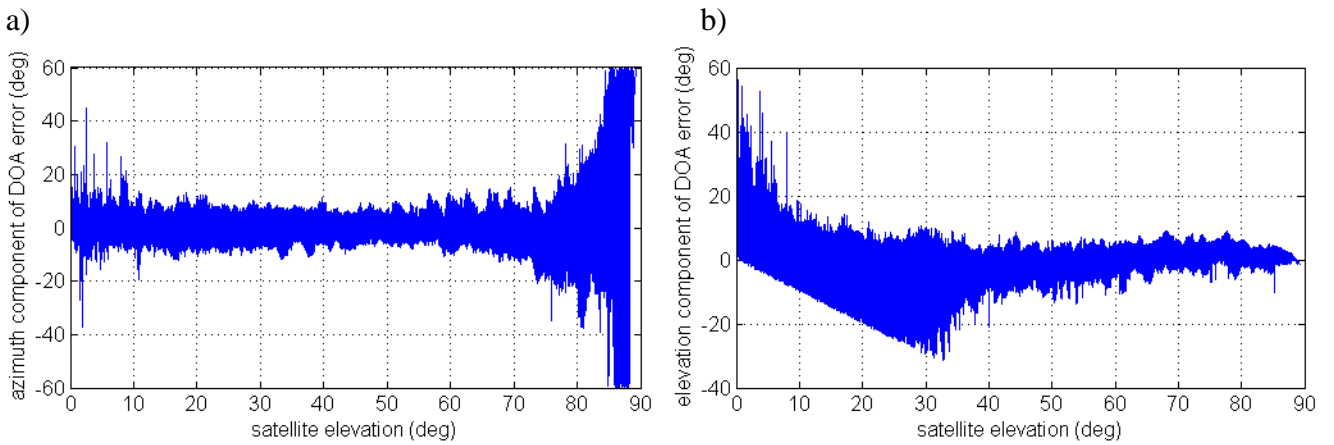


Fig. 4 Overview of DOA estimation error vs. elevation; a) azimuth component, b) elevation component

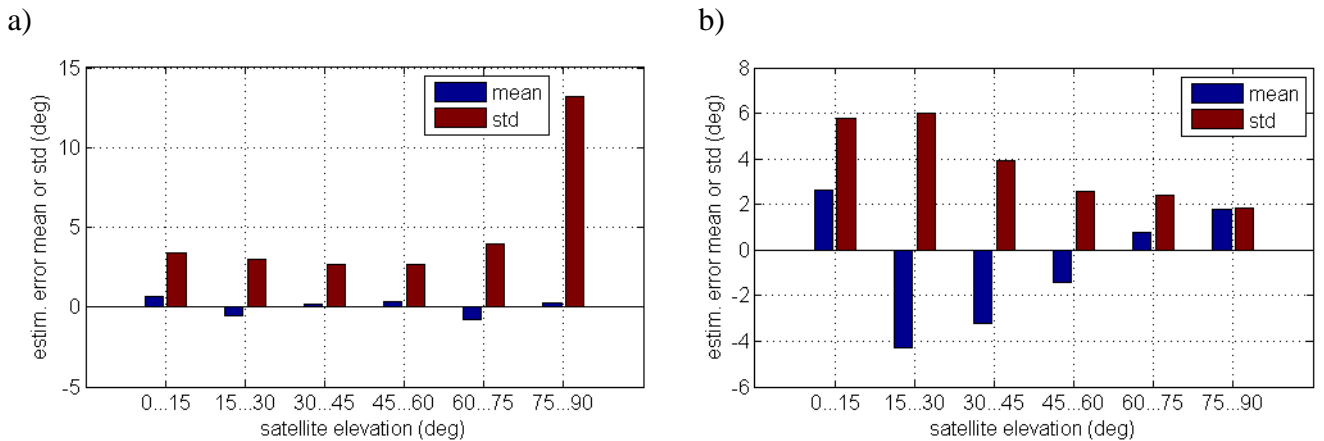


Fig. 5 Statistical description of DOA estimation error vs. elevation; a) azimuth component, b) elevation component

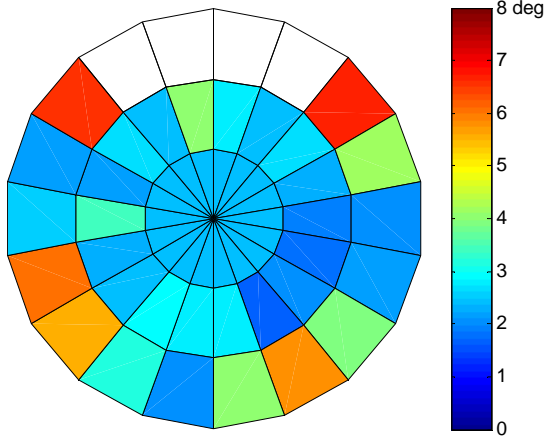


Fig. 6 Angular RMSE of DOA estimation

In (8) the variable θ denotes the satellite elevation in degrees and σ_{90} the standard deviation of the DOA estimation error in zenith. The latter depends on various side conditions like the signal-to-noise ratio of the signal for which the DOA is estimated etc. Moreover, the model (8) depends on the parameter K which characterizes how strongly the DOA estimation error varies with elevation.

For the set of measurement data analyzed within the paper the zenith DOA estimation error σ_{90} was 2.3364° and the parameter K was one. The fit of this model to the observed DOA estimation error is shown in Fig. 7a). By varying the choice for the parameter K also antennas can be described with weaker or stronger dependency of the DOA estimation error on elevation. This will later be used within our analysis to quantify the sensitivity of the considered algorithms with respect to this elevation dependency. This generalized model of the DOA estimation error is depicted in Fig. 7b).

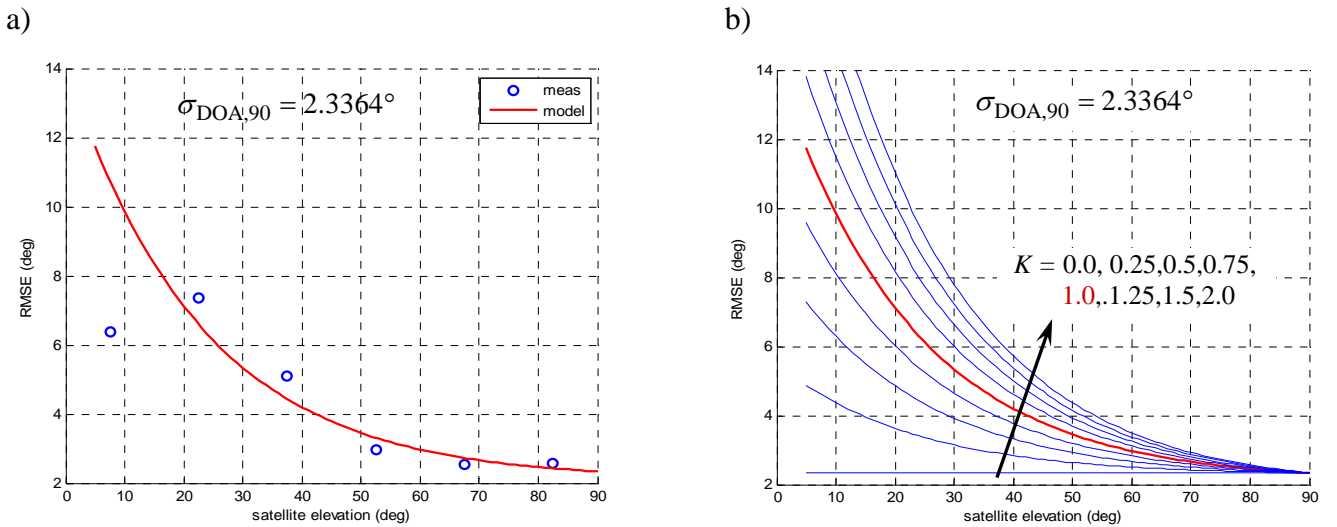


Fig. 7 Derived model for DOA estimation error; a) fitting curve for measurement data, b) generalized version

IV. Extended Antenna Based Joint Attitude Estimation and Spoofing Detection

A. Novel Technique for Spoofing Detection

1. Mathematical derivation and description

As shown in Section III the quality of DOA estimation results significantly differ among the satellite signals. The main influence seen is related to the elevation in the local antenna coordinate system under which the satellite signal is received. The technique revisited in Section II cannot cope with these side conditions. Therefore, setting out from the results of Section II it is the purpose of this section to present a novel extended technique for joint attitude estimation and spoofing detection which can take different qualities of DOA estimation results into account.

Coming back to (2) the impact of DOA estimation errors can be described by rotation noise according to

$$\hat{\mathbf{b}}_n = \mathbf{R}_n^N \underbrace{\mathbf{R}(r, p, y)}_{=\mathbf{b}_n} \mathbf{a}_n, \quad 1 \leq n \leq N. \quad (9)$$

We assume, that the DOA estimation error

$$\mathbf{n}_{b,n} = \hat{\mathbf{b}}_n - \mathbf{b}_n, \quad (10)$$

is small, i.e. $\|\mathbf{n}_{b,n}\| \ll 1$ holds. In this case the nonlinear transformation $\hat{\mathbf{b}}_n = \mathbf{R}_n^N \mathbf{b}_n$ for expressing the rotational noise can be well approximated by linear Taylor approximation according to

$$\hat{\mathbf{b}}_n = \mathbf{b}_n + \mathbf{B}_{\perp,n} \mathbf{n}_n. \quad (11)$$

In (11) the matrix $\mathbf{B}_{\perp,n}$ describes a local set of basis vectors corresponding to the true DOA expressed by \mathbf{b}_n , which span a local coordinate system. In this local coordinate system the first component is in direction of local azimuth, the second one in direction of local elevation and the third one in radial direction, see Fig. 8. The error vector \mathbf{n}_n in (11) expresses the DOA error components in azimuth, elevation and radial direction and is measured in radian.

The covariance matrix of the error vector \mathbf{n}_n of (11) reads

$$\mathbf{C}_{n,n} = E\{\mathbf{n}_n \mathbf{n}_n^T\}, \quad (12)$$

where $[\mathbf{C}_{n,n}]_{1,1}$ is the variance of the azimuth error, $[\mathbf{C}_{n,n}]_{2,2}$ the variance of the elevation error and $[\mathbf{C}_{n,n}]_{3,3}$ the variance in radial direction. The variance in radial direction is much smaller than the variances in azimuth and elevation direction since rotational noise mainly influences the azimuth and elevation components of the DOA estimation error $\mathbf{n}_{b,n}$ of (10). Stacking equations (11) for all satellite signals $n = 1 \dots N$ one obtains

$$\text{vec}\{\widehat{\mathbf{B}}\} = \text{vec}\{\mathbf{B}\} + \mathbf{B}_{\perp} \mathbf{n}. \quad (13)$$

In (13) “ $\text{vec}\{\cdot\}$ ” denotes the vectorial operator. This operator takes a matrix as argument and outputs a vector, which is constituted by stacking all columns of the matrix. Moreover also the matrix

$$\mathbf{B}_{\perp} = \text{blockdiag}(\mathbf{B}_{\perp,1} \dots \mathbf{B}_{\perp,N}) \quad (14)$$

and the error vector

$$\mathbf{n} = (\mathbf{n}_1^T \dots \mathbf{n}_N^T)^T \quad (15)$$

are obtained by combining the satellite specific quantities. The covariance matrix of the combined error vector \mathbf{n} of (15) reads

$$\mathbf{C}_n = \text{blockdiag}(\mathbf{C}_{n,1} \dots \mathbf{C}_{n,N}). \quad (16)$$

In the following we assume that the DOA estimation error measured in the local coordinate system of Fig. 4 is Gaussian distributed. In this case the probability distribution of \mathbf{n} of (15) can be described by the generalized multivariate Gaussian distribution

$$p_n(\mathbf{n}) = \frac{1}{\sqrt{2\pi}^{3N} \det(\mathbf{C}_n)} e^{-\frac{1}{2}(\mathbf{n}-\boldsymbol{\mu})^T \mathbf{C}_n^{-1} (\mathbf{n}-\boldsymbol{\mu})}, \quad (17)$$

where \mathbf{C}_n is the covariance matrix of (16) and $\boldsymbol{\mu}$ is the vector describing the mean of the distribution. Setting out from the results of Fig. 5 we can conclude that the mean is close to zero and can, therefore, be neglected in the following.

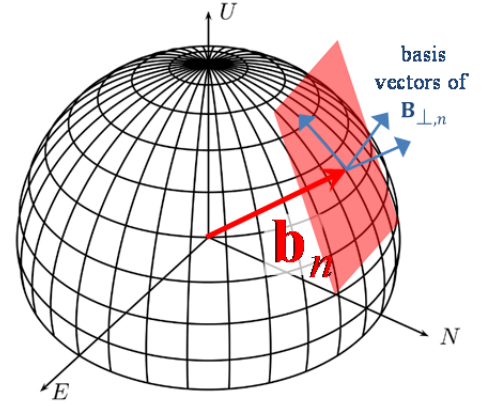


Fig. 8 Definition of a local set of basis vectors

Based on the DOA estimation error distribution of (17) the maximum likelihood estimate (ML estimate)

$$(\hat{r}, \hat{p}, \hat{y}) = \arg \max_{\nu(r,p,y)} p(\widehat{\mathbf{B}}|r, p, y) \quad (18)$$

of the unknown Euler angles r , p and y can be defined. Using (13) one obtains

$$p(\widehat{\mathbf{B}}|r, p, y) = p_n(\mathbf{n} = \mathbf{B}_{\perp}^{-1} \text{vec}\{\widehat{\mathbf{B}} - \mathbf{R}(r, p, y)\mathbf{A}\}) \quad (19)$$

Substituting (17) and (19) in (18) we get

$$(\hat{r}, \hat{p}, \hat{y}) = \arg \min_{\nu(r,p,y)} \text{vec}^T\{\widehat{\mathbf{B}} - \mathbf{R}(r, p, y)\mathbf{A}\} \cdot \underbrace{\mathbf{B}_{\perp}^{-1T} \mathbf{C}_n^{-1} \mathbf{B}_{\perp}^{-1}}_{=c^{-1}} \text{vec}\{\widehat{\mathbf{B}} - \mathbf{R}(r, p, y)\mathbf{A}\} \quad (20)$$

as the final result for the ML estimate of the Euler angles, which takes the individual quality of the DOA estimation errors into account. The solution of (20) can be determined following an iterative approach as described in [2].

2. Special cases of the novel technique

Let's for a moment have a look onto two special cases of (20). First let's consider uncorrelated, identically and isotropically distributed noise. In this case \mathbf{C}_n of (16) is a scaled identity matrix. Plugging this choice for \mathbf{C}_n into (20) one obtains

$$\begin{aligned} (\hat{r}, \hat{p}, \hat{y}) &= \arg \min_{\nu(r,p,y)} \text{vec}^T\{\widehat{\mathbf{B}} - \mathbf{R}(r, p, y)\mathbf{A}\} \cdot \\ &\quad \text{vec}\{\widehat{\mathbf{B}} - \mathbf{R}(r, p, y)\mathbf{A}\} \\ &= \arg \min_{\nu(r,p,y)} \|\widehat{\mathbf{B}} - \mathbf{R}(r, p, y)\mathbf{A}\|_2^2. \end{aligned} \quad (21)$$

The result of (21) is identical to the result of (4), i.e. for the considered special case the generalized novel technique proposed in this section converges towards the state-of-the-art technique revisited in Section II.

Let's now have a look onto the more realistic and relevant case in which individual satellite signals show different levels of error in the DOA estimation. We assume that for the covariance matrix $\mathbf{C}_{n,n}$ of (12) for satellite signal n

$$\mathbf{C}_{n,n} = \sigma_n^2 \mathbf{I}^{(3 \times 3)} \quad (22)$$

holds. From (22) follows for the covariance matrix of the combined error vector of (16)

$$\mathbf{C} = \underbrace{\begin{pmatrix} \sigma_1^2 & 0 & 0 \\ 0 & \ddots & 0 \\ 0 & 0 & \sigma_N^2 \end{pmatrix}}_{=\mathbf{W}^{-2}} \otimes \mathbf{I}^{(3 \times 3)}. \quad (23)$$

In (23) the symbol “ \otimes ” denotes the Kronecker product of matrices and vectors. Substituting (23) in (20) one obtains

$$\begin{aligned} (\hat{r}, \hat{p}, \hat{y}) &= \arg \min_{\mathbf{v}(r,p,y)} \text{vec}^T \{ (\hat{\mathbf{B}} - \mathbf{R}(r,p,y)\mathbf{A})\mathbf{W} \} \cdot \\ &\quad \text{vec} \{ (\hat{\mathbf{B}} - \mathbf{R}(r,p,y)\mathbf{A})\mathbf{W} \} \\ &= \arg \min_{\mathbf{v}(r,p,y)} \| (\hat{\mathbf{B}} - \mathbf{R}(r,p,y)\mathbf{A})\mathbf{W} \|_2^2 \end{aligned} \quad (24)$$

for the ML estimate. By some matrix arithmetics (24) can be further simplified to

$$(\hat{r}, \hat{p}, \hat{y}) = \arg \min_{\mathbf{v}(r,p,y)} \text{trace} \left\{ \mathbf{W}^T (\hat{\mathbf{B}} - \mathbf{R}(r,p,y)\mathbf{A})^T (\hat{\mathbf{B}} - \mathbf{R}(r,p,y)\mathbf{A}) \mathbf{W} \right\} \quad (25)$$

and

$$\begin{aligned} \hat{\mathbf{R}} &= \arg \max_{\mathbf{R} \in \text{SO}(3)} \text{trace} \left\{ (\hat{\mathbf{B}}\mathbf{W})^T \mathbf{R}(r,p,y)\mathbf{A}\mathbf{W} \right\} \\ &= \arg \max_{\mathbf{R} \in \text{SO}(3)} \text{trace} \left\{ \underbrace{\mathbf{A}\mathbf{W}(\hat{\mathbf{B}}\mathbf{W})^T}_{=\mathbf{D}} \mathbf{R}(r,p,y) \right\}. \end{aligned} \quad (26)$$

The matrix \mathbf{D} in (26) reads

$$\mathbf{D} = \mathbf{A}\mathbf{W}\mathbf{W}^T\hat{\mathbf{B}}^T = \mathbf{A} \begin{pmatrix} \sigma_1^2 & 0 & 0 \\ 0 & \ddots & 0 \\ 0 & 0 & \sigma_N^2 \end{pmatrix} \hat{\mathbf{B}}^T. \quad (27)$$

Solving (26) using the method of Langragian multipliers yields

$$\hat{\mathbf{R}} = \mathbf{D}^T (\mathbf{D}\mathbf{D}^T)^{-\frac{1}{2}} \quad (28)$$

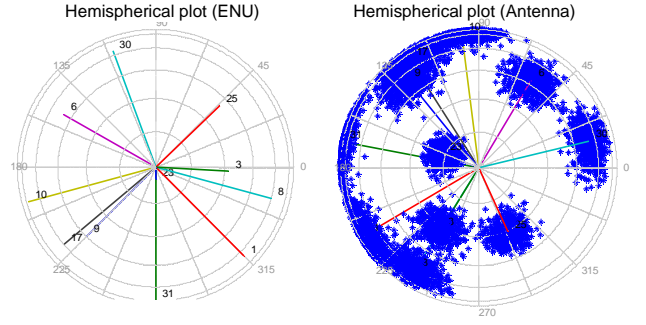


Fig. 9 Considered scenario with 11 satellites

for the optimum rotation matrix. Using the singular value decomposition

$$\mathbf{D} = \mathbf{A}\mathbf{W}\mathbf{W}^T\hat{\mathbf{B}}^T = \mathbf{U}\mathbf{\Sigma}\mathbf{V}^T \quad (29)$$

of \mathbf{D} of (27) one obtains a closed-form solution

$$\hat{\mathbf{R}} = \mathbf{V} \text{diag}(1, 1, \det(\mathbf{U}\mathbf{V}^T)) \mathbf{U}^T. \quad (30)$$

The optimum Euler angles can be determined based on the optimum rotation matrix by [11]

$$\tan \hat{r} = -\frac{[\hat{\mathbf{R}}]_{1,3}}{[\hat{\mathbf{R}}]_{3,3}}, \quad \tan \hat{p} = -\frac{[\hat{\mathbf{R}}]_{2,3}}{\sqrt{[\hat{\mathbf{R}}]_{2,1}^2 + [\hat{\mathbf{R}}]_{2,2}^2}}, \quad (31)$$

$$\tan \hat{y} = -\frac{[\hat{\mathbf{R}}]_{2,1}}{[\hat{\mathbf{R}}]_{2,2}}.$$

Equation (30) in combination with (27) and (31) describes the optimum technique for joint spoofing detection and attitude estimation if the quality of the DOA estimation errors differs among satellite signals.

B. Analysis Results

The performance of the new technique is analyzed by means of Monte Carlo computer simulations. A scenario with 11 satellites is considered, see Fig. 9. The unknown antenna attitude to be estimated is

$$r = 10^\circ, p = 5^\circ, y = 100^\circ. \quad (32)$$

For the simulation scenario the standard deviation of the DOA estimation error was chosen in accordance to the generalized model of (8). We varied the choice of parameter K in wide ranges in order to study the influence of different types of antennas with different elevation dependency on the analysis results. Fig. 10 shows the resulting error in attitude determination as a function of the parameter K .

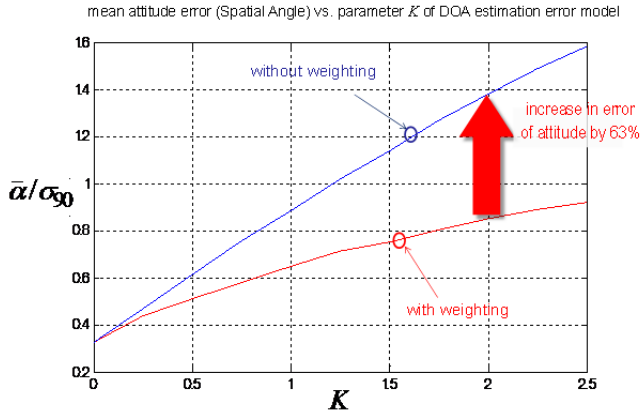


Fig. 10 Mean attitude error (spatial separation angle) vs. parameter K of the generalized error model

The improvements achievable by considering weighting during the attitude determination step can be clearly seen.

C. Spoofing Mitigation using Spatial Processing

In a multi antenna receiver the impact of spoofing can be mitigated by spatial processing [3]. For this purpose nulls in the antenna diagram can be steered to suppress the influence of identified spoofing sources. If the direction to the spoofing source has been estimated by means of the techniques described in the sections above, the spatial zero can be generated by applying an orthogonal projection Π_{\perp} into the null sub-space of the array steering vector $\mathbf{a}(\theta, \varphi)$ that corresponds to the spoofer direction

$$\begin{aligned} \Pi_{\perp} &= \mathbf{I} - \mathbf{a}(\mathbf{a}^H \mathbf{a})^{-1} \mathbf{a}^H, \\ \hat{\mathbf{x}}[n] &= \Pi_{\perp} \mathbf{x}[n], \end{aligned} \quad (33)$$

where $\mathbf{x}[n]$ stands for the array output vector at correlation epoch n .

In the following this approach is validated by means of the DLR multi antenna receiver GALANT [18]. The setup and configuration is similar to the one described in Section III. Besides the null steering described above, an Eigenbeam-forming approach was utilized to generate the antenna array weights [17], i.e. for adapting the reception pattern of the antenna array. The GPS constellation at the start of recording of the IF samples is shown in Fig. 11. A GNSS repeater was used to inject spoofed / repeated signals from boresight direction.

Fig. 12 shows examples of the normalized array reception patterns in different satellite channel without and with the spatial null. It can clearly be seen how the spoofed signal is suppressed by applying spatial processing.

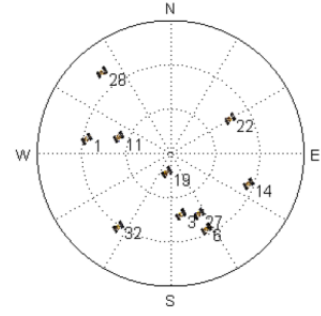


Fig. 11 GPS constellation at start of signal recording

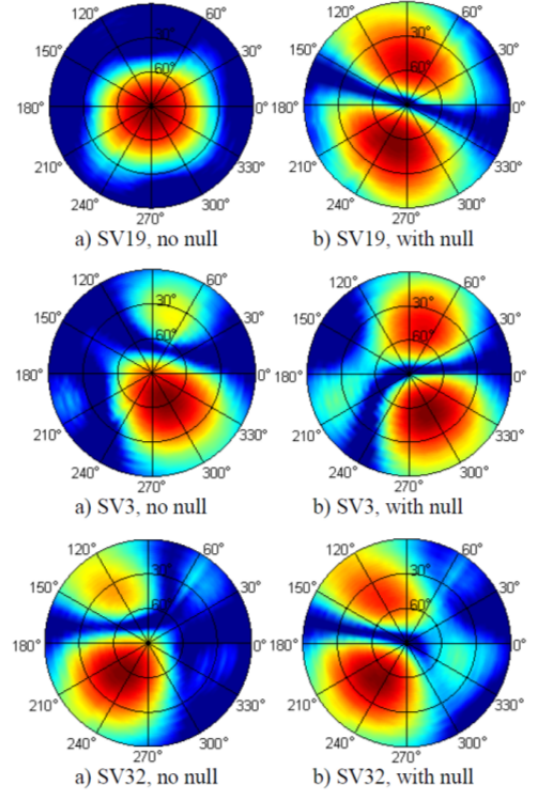


Fig. 12 Examples of array reception pattern without and with spatial null

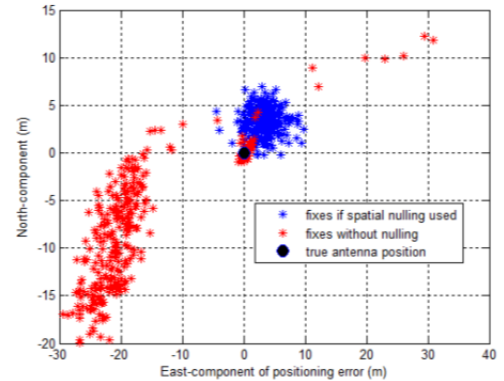


Fig. 13 Planar positioning error under spoofing conditions with and without adaptive nulling

In Fig. 13 the resulting solutions in the position domain are shown. Without placing spatial nulls the impact of the spoofer / repeater on the position is clearly visible. In case of activated spatial nulling the systematic position error caused by the spoofer is avoided and accurate position estimates are determined.

V. Sequential Processing

A. Sequential Technique for Spoofing Detection

In typical scenarios in mobility on land, on sea and in the air, the attitude of the user platform (e.g. vehicle, ship, aircraft) does not change suddenly but with limited turn rates and turn rate changes. Therefore, the knowledge about attitude in a certain epoch can be exploited for the attitude estimation in following epochs as a priori knowledge. In this section, the snapshot based techniques introduced in the previous sections will be further extended to a new sequential technique for joint spoofing detection and attitude estimation which exploits the limited changes in attitude.

For that purpose we introduce the state vector

$$\mathbf{x}_k = \begin{pmatrix} r \\ p \\ y \\ \dot{r} \\ \dot{p} \\ \dot{y} \end{pmatrix} \quad (34)$$

which contains the three Euler angles r , p , y describing the attitude of the antenna platform as well as the corresponding turn rates \dot{r} , \dot{p} and \dot{y} . With the time T describing the duration of one measurement and update interval the state transition model

$$\mathbf{x}_k = \begin{pmatrix} 1 & 0 & 0 & T & 0 & 0 \\ 0 & 1 & 0 & 0 & T & 0 \\ 0 & 0 & 1 & 0 & 0 & T \\ 0 & 0 & 0 & 1 & 0 & 0 \\ 0 & 0 & 0 & 0 & 1 & 0 \\ 0 & 0 & 0 & 0 & 0 & 1 \end{pmatrix} \mathbf{x}_{k-1} + \mathbf{w}_k \quad (35)$$

can be introduced describing the change in attitude from update step $k-1$ to k . In (35) the vector \mathbf{w}_k denotes the process noise. The relationship between the measurements $\hat{\mathbf{B}}$ of (13) and the state vector \mathbf{x}_k of (34) is modelled by the non-linear measurement model

$$\tilde{\mathbf{z}}_k = \text{vec}\{\hat{\mathbf{B}}\} = \mathbf{h}(\mathbf{x}_k, \mathbf{v}_k) = \mathbf{R}_c \text{vec}\{\mathbf{A}\} \quad (36)$$

using the measurement noise vector \mathbf{v}_k , where

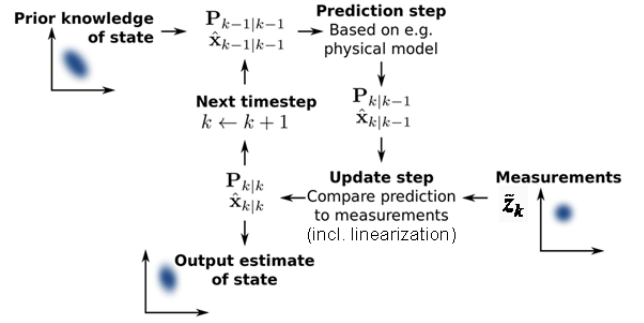


Fig. 14 Steps of the Extended Kalman filter [19] using the state transition model of (35) and the measurement model of (36)

$$\mathbf{R}_c = \text{blockdiag}(\mathbf{R}_{c,1} \dots \mathbf{R}_{c,N}), \quad (37)$$

$$\mathbf{R}_{c,n} = \mathbf{R}(r(\mathbf{x}_k) + n_{r,n}, p(\mathbf{x}_k) + n_{p,n}, y(\mathbf{x}_k) + n_{y,n}).$$

Equations (34) to (37) describe an extended Kalman filter which can be evaluated by means of the standard steps depicted in Fig. 14 and detailed in [19]. The analysis of achievable performance gains by going from a snapshot based to a sequential technique is subject to further research and will be presented in the next paper.

VI. Conclusions and Outlook

It was shown in the paper that the estimation error in direction-of-arrival (DOA) estimation are highly dependent on the DOA to be estimated. Therefore, it is highly advised to incorporate the knowledge about differences in the quality of DOA estimates in a joint spoofing detection and attitude estimation process. It was shown in the paper that the approaches for joint spoofing detection and attitude estimation known from literature can be generalized to cope with this new side information. Corresponding improvement gains can be achieved.

Since attitude cannot change suddenly over time further improvements can be gained by extending the proposed generalized approach to a sequential technique. As shown in the paper this extension can be achieved by following an extended Kalman filter based approach.

Using the history of attitude changes as well as about spoofed and unspoofed subsets of GNSS signals allows further reducing the complexity of the overall process. Having knowledge about trustful GNSS signal subsets from previous epochs as well as about spoofed signal subsets allows breaking down the average number of hypotheses to be tested in the process significantly. The detailed analysis of this potential for complexity reduction is subject of further research.

ACKNOWLEDGEMENTS

Parts of the research leading to the results reported in this paper have been funded within the project KOSERNA by the German Aerospace Center (DLR) on behalf of the German Federal Ministry of Economics and Technology under grant no. 50 NA 1406. This support is greatly acknowledged.

REFERENCES

- [1] T. E. Humphreys, B. M. Ledvina, M. L. Psiaki, B. W. O'Hanlon, and P. M. Kintner Jr, "Assessing the spoofing threat: Development of a portable GPS civilian spoofer," Proceedings of the ION GNSS international technical meeting of the satellite division, vol. 55, p. 56, 2008.
- [2] M. Meurer, A. Konovaltsev, M. Cuntz, and C. Hättich, "Robust Joint Multi-Antenna Spoofing Detection and Attitude Estimation using Direction Assisted Multiple Hypotheses RAIM," in Proc. ION GNSS 2012, 2012.
- [3] A. Konovaltsev, M. Cuntz, C. Haettich, and M. Meurer, "Autonomous Spoofing Detection and Mitigation in a GNSS Receiver with an Adaptive Antenna Array," in Proc. ION GNSS+ 2013, 2013.
- [4] M. Appel, A. Konovaltsev, and M. Meurer, "Robust Spoofing Detection and Mitigation based on Direction of Arrival Estimation," in Proc. ION GNSS+ 2015, 2015.
- [5] K. Wesson, D. Shepard, and T. Humphreys, "Straight talk on antispoofing: Securing the future of PNT," GPS World, vol. 23, no. 1, 2012.
- [6] A. Jafarnia-Jahromi, A. Broumandan, J. Nielsen, and G. Lachapelle, "GPS vulnerability to spoofing threats and a review of antispoofing techniques," International Journal of Navigation and Observation, vol. 2012, 2012.
- [7] P. Y. Montgomery, T. E. Humphreys, and B. M. Ledvina, "A multiantenna defense: Receiver-autonomous GPS spoofing detection," Inside GNSS, vol. 4, no. 2, pp. 40–46, 2009.
- [8] M. Cuntz, L. Greda, M. Heckler, A. Konovaltsev, M. Meurer, L. Kurz, G. Kappen, and T. Noll, "Lessons learnt: The development of a robust multi-antenna GNSS receiver," Proc. ION GNSS 2010, pp. 21–24, 2010.
- [9] R. Roy, "ESPRIT-estimation of signal parameters via rotational invariance techniques," IEEE Transactions on Acoustics, Speech and Signal Processing, vol. 37, no. 7, pp. 984–995, 1989.
- [10] M. Haardt, "Efficient One-, Two-, and Multidimensional High-Resolution Array Signal Processing," Ph.D. dissertation, Technical University of Munich, 1997.
- [11] B. Hofmann-Wellenhof et al, GNSS - Global Navigation Satellite Systems: GPS, GLONASS, Galileo, and more. Wien: Springer-Verlag, 2007.
- [12] F. Markley, "Attitude determination using vector observations and the singular value decomposition," The Journal of the Astronautical Sciences, vol. 38, no. 3, pp. 245–258, 1988.
- [13] G. Volpe Center, "Vulnerability report", 2001.
- [14] L. Scott, "Anti-spoofing & authenticated signal architectures for civil navigation systems", in Proc. of the 16th International Technical Meeting of the Satellite Division of The Institute of Navigation (ION GPS/GNSS 2003), pp. 1543-1552, 2003.
- [15] G. W. Hein, F. Kneisl, J.-A. Avila-Rodriguez, and S. Wallner, "Authenticating GNSS, proofs against spoofs, part 1", Inside GNSS, vol. 2, no. 4, pp. 58–63, 2007.
- [16] G. W. Hein, F. Kneisl, J.-A. Avila-Rodriguez, and S. Wallner, "Authenticating GNSS, proofs against spoofs, part 2", Inside GNSS, vol. 2, no. 5, pp. 71–78, 2007.
- [17] M. Sgammini, F. Antreich, L. Kurz, M. Meurer, and T. G. Noll, "Blind Adaptive Beamformer Based on Orthogonal Projections for GNSS," in 25th International Technical Meeting of The Satellite Division of the Institute of Navigation - ION GNSS, 2011, no. 1.
- [18] M. V. T. Heckler, M. Cuntz, A. Konovaltsev, L. A. Greda, A. Dreher, and M. Meurer, "Development of Robust Safety-of-Life Navigation Receivers," IEEE Transactions on Microwave Theory and Techniques, vol. 59, no. 4, pp. 998–1005, Apr. 2011.
- [19] https://en.wikipedia.org/wiki/Kalman_filter
- [20] S. J. Julier, S.J., J.K. Uhlmann, "Unscented filtering and nonlinear estimation". Proceedings of the IEEE, pp. 401-422, 2004.